Simple and efficient method for specularity removal in an image

Hui-Liang Shen* and Qing-Yuan Cai

Department of Information and Electronic Engineering, Zhejiang University, Hangzhou 310027, China

*Corresponding author: shenhl@zju.edu.cn

For dielectric inhomogeneous objects, the perceived reflections are the linear combinations of diffuse and specular reflection components. Specular reflection plays an important role in the fields of image analysis, pattern recognition, and scene synthesis. Several methods for the separation of the diffuse and the specular reflection components have been presented based on image segmentation or local interaction of neighboring pixels. We propose a simple and effective method for specularity removal in a single image on the level of each individual pixel. The chromaticity of diffuse reflection is approximately estimated by employing the concept of modified specular-free image, and the specular component is adjusted according to the criterion of smooth color transition along the boundary of diffuse and specular regions. Experimental results indicate that the proposed method is promising when compared with other state-of-the-art techniques, in both separation accuracy and running speed. © 2009 Optical Society of America

OCIS codes: 100.3020, 100.2960, 330.1690.

1. Introduction

In the fields of image processing and computer vision, many algorithms assume that the object surfaces are purely diffuse, and some of these algorithms will become erroneous if this assumption is violated. Inhomogeneous materials, including plastic, wood, polyester, and human skin, always have both diffuse and specular reflection components in the real world. To obtain pure diffuse reflection, the specularity needs to be accurately removed. The separated specular reflection component could be further used to estimate surface roughness and lighting direction [1,2] or for image-based scene synthesis [3].

The diffuse and specular reflections are described as follows. When a ray of light strikes the surface of an inhomogeneous material, part of the ray is immediately reflected from the interface between the surface and the air owing to their different refractive indices. This part of the light ray is termed specular reflection, which is dependent on the local orientation and roughness degree of the surface. The remainder of the ray penetrates the surface and enters the body of the material. A part of this light is absorbed by the colorant and the medium, while other light arrives back at the surface and reenters the air. The latter is referred as diffuse reflection. The spectral composition of the diffuse reflection describes the spectral characteristic of the material, and the spectral power distribution of the specular reflection is very similar to that of the illuminant [4]. According to the dichromatic reflection model [5], the perceived reflection is the linear combination of these two components.

A. Previous Work

Many methods have been proposed to separate these two components. Based on the observation that the specular reflection is polarized while the diffuse reflection is not; Nayar *et al.* [6] proposed to separate reflection components from color images by placing a polarization filter in front of the imaging sensor. Their method can deal with highlights on an object surface with heavy textures and nonconstant diffuse

components, as well as different material properties. Klinker *et al.* [7] found that, for a single-colored object surface, the color histogram of the image forms a skewed T-shaped distribution with two limbs. They proposed an algorithm to identify these two limbs and then separate the diffuse and specular components for each pixel.

Tan and Ikeuchi [8] presented a method to remove specularity in a single-textured color image. Their work introduces a specular-to-diffuse mechanism and the concept of specular-free (SF) image. The SF image has only diffuse reflection but keeps the same geometrical distribution of the original image. The pixels containing pure diffuse reflection can be identified by the logarithmic differentiation operation on the original and SF images. Then the specularity of a highlight pixel can be reduced by iteratively shifting the maximum chromaticity to that of a more diffuse neighboring pixel. Some different forms of SF image have also been introduced in the literature [9–12]. Miyazaki *et al.* [9] generated the SF image by using a special color space and substituting the saturation component into the intensity component. Yoon *et al.* [10] obtained a SF two-band image by subtracting the minimum RGB value from each channel for each pixel. Shen *et al.* [11] proposed the concept of modified SF (MSF) image to reduce the noise influence on chromaticity. Their method works in an iterative manner, by selecting appropriate body color and separating reflection components of pixels with similar chromaticity under the least-squares criterion. Shen *et al.* [12] presented a one-channel SF image calculation method for photometric stereo techniques. Tan *et al.* [13] proposed a method to separate the diffuse and the specular reflection components of uniformly colored object surfaces based on the maximum chromaticity–intensity space and the analysis of camera noises. By assuming that the spectral sensitivity of the camera is known, Tan and Ikeuchi [14] further proposed the decomposition of reflection components by using a series of linear basis functions.

Mallick *et al.* [15] presented a framework to remove the specular reflection component of a multicolored surface from a single image or video sequence. Starting from an illumination-aligned color space that contains specular reflection in one axis and pure diffuse reflections in the remaining two axes [16], the specularity removal is accomplished by using a partial differential equation that iteratively erodes the specular component. Park and Lee [17] proposed a method to inpaint highlight by using two images with different exposure times, based on the color line projection technique. Tan *et al.* [18] proposed an illumination-constrained inpainting method to remove the specular reflection in the manually identified highlight region. Compared with traditional image inpainting techniques, this method can recover better surface texture and shading intensities. Lin and Lee [1] used four photometric images to separate reflection components, estimate surface roughness, and construct new reflection appearance.

It is noted that although the above methods can separate the diffuse and specular reflection components from images or videos, they all have limitations. The work by Nayar could produce reliable results [6], but using additional polarization filters is not practical in many real imaging systems. Some methods can only remove specularity from objects with the same diffuse color, and preprocessing steps such as image segmentation is necessary when dealing with multicolored surfaces [7,13]. Some other methods are able to handle the separation of specular reflection from textured and multicolored surfaces by considering the interactions between neighboring pixels [8,14,15,17,18]. However, as an iterative framework is adopted or complicated local interactions are utilized in these methods, these algorithms may become time consuming.

B. Our Contribution

As specularity removal sometimes works as a preprocessing step for other algorithms in the field of computer vision, it is desired that the method be of low complexity and high efficiency. This paper proposes such a method to separate the diffuse and specular reflection components for multicolored texture surfaces by using a single image. Similar to many of previous methods, the following assumptions are used in the proposed method: (1) the dichromatic reflection model is applicable, (2) the camera responses are linear to the light flux entering the sensor, and (3) the color of the illuminant is known *a priori* or can be estimated by using color constancy algorithms [19].

The proposed method works in a pixelwise manner, or equivalently, the separation of diffuse and specular reflection components is conducted on each individual pixel without region segmentation and even the local interaction between pixels. In this way the running speed of the proposed method depends only on the image size, almost irrelevant to the complexity level of the image content.

In the proposed method, the SF image is generated by subtracting the minimum RGB value for each pixel. The SF image keeps the same geometrical orientation of the original image, while the chromaticity may be biased. A mechanism is introduced to add an offset onto the SF image so that its chromaticity is closer to that of the diffuse component. After the candidate specular component is obtained by a simple thresholding operation, it is further tuned so that the separated diffuse and specular reflection components are more reasonable for different kinds of materials.

C. Paper Organization

The remainder of the paper is organized as follows. Section 2 discusses the dichromatic reflection model in the spectral reflectance space and RGB color space. In Section 3, we present the proposed specularity separation method, including the generation of the SF image, the chromaticity analysis, and the calculation of the specular reflection component.
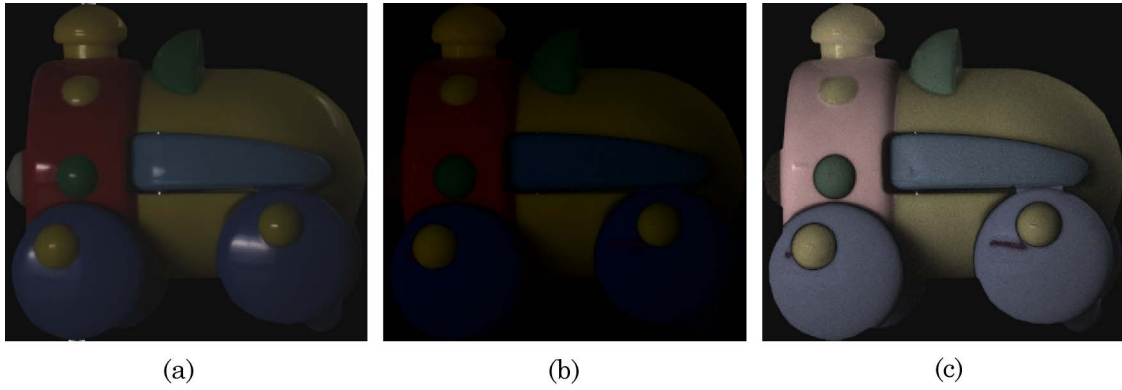
Fig. 1. (Color online) Two different SF images. (a) Original train image, (b) SF image of the proposed method, (c) SF image of Tan's method [8].

Experimental results and associated discussion are provided in Section 4. Finally, Section 5 concludes the paper.

2. Formulation of the Reflection Model

In this paper, we assume that the color camera behaves in a linear manner, which means that the RGB response values are proportional to the intensity of the light entering the sensor. Let V_i denote the response of the ith channel ($i = 1, 2, 3$, or equivalently, red, green, blue) and $r(\lambda, p)$ represent the spectral reflectance of wavelength λ at pixel position p, $l(\lambda)$ be the spectral power distribution of the illuminant, and $s_i(\lambda)$ be the spectral sensitivity of the ith channel of the camera; then the imaging process can be formulated as

$$V_i(p) = \int r(\lambda, p)l(\lambda)s_i(\lambda)\mathrm{d}\lambda, \tag{1}$$

where the integral is applied in the visible wavelength range.

According to the dichromatic reflection model, the reflection of inhomogeneous material consists of diffuse reflection and specular reflection; each can be further decomposed into two independent components, i.e., spectral and geometrical:

$$r(\lambda, p) = \alpha(p)r_b(\lambda) + \beta(p)r_s(\lambda), \tag{2}$$

where $r_b(\lambda)$ and $r_s(\lambda)$ denote the wavelength composition of the diffuse and the specular reflectance, respectively, and $\alpha(p)$ and $\beta(p)$ are the geometrical factors of these two reflections at pixel p, respectively. As the spectral power distribution of the specular reflection component is similar to that of the illuminant [5], $r_s(\lambda)$ is independent of wavelength λ, and Eq. (2) can be written as

$$r(\lambda, p) = \alpha(p)r_b(\lambda) + \beta(p)r_s. \tag{3}$$

Substituting Eq. (3) into Eq. (1) yields

$$V_i(p) = \alpha(p)\int_\lambda r_b(\lambda)l(\lambda)s_i(\lambda)\mathrm{d}\lambda + \beta(p)r_s\int_\lambda l(\lambda)s_i(\lambda)\mathrm{d}\lambda$$
$$= \alpha(p)V_{b,i} + \beta(p)V_{s,i}, \tag{4}$$

where $V_{b,i} = \int_\lambda r_b(\lambda)l(\lambda)s_i(\lambda)\mathrm{d}\lambda$ is the intrinsic body color of the material and $V_{s,i} = r_s\int_\lambda l(\lambda)s_i(\lambda)\mathrm{d}\lambda$ denotes the illuminant color. In this study, the illuminant color is acquired by imaging a pure white panel. The color of each pixel is then normalized with respect to the illuminant color and rescaled into the range from 0 to 255. In this way, $V_{s,i} = 255$ for each channel, and Eq. (4) becomes

$$V_i(p) = \alpha(p)V_{b,i} + \beta_s(p), \tag{5}$$

where $\beta_s(p) = \beta(p)V_{s,i} = 255\beta(p)$.

3. Proposed Method

We obtain our SF image by subtracting the minimum RGB value for each pixel and adding an offset so that the chromaticity of the modified spectral-free image is close to that of the diffuse component. The specular component can then be adjusted under the criterion of continuous color distribution.

A. Specular-Free Image and Chromaticity

The concept of a SF image, which refers to an image that does not contain the specular component, was first introduced by Tan and Ikeuchi [8]. The characteristic of their SF image is that it maintains the geometrical information of the diffuse component, but the color distribution is different. In their work, the SF image is formed by setting the diffuse maximum chromaticity equal to a constant scalar value (for example, 0.5) for all pixels.

Alternatively, we present a much simple way to generate an appropriate SF image:

$$V_{\mathrm{SF},i}(p) = V_i(p) - V_{\min}(p), \tag{6}$$

where $V_{\min}(p) = \min_i\{V_i(p)\}$. It is noted that this SF image calculation was also adopted in previous work [10–12]. As $V_{\min}(p)$ can be represented by the dichromatic reflection model as

$$V_{\min}(p) = \alpha(p)V_{b,\min} + \beta_s(p), \tag{7}$$
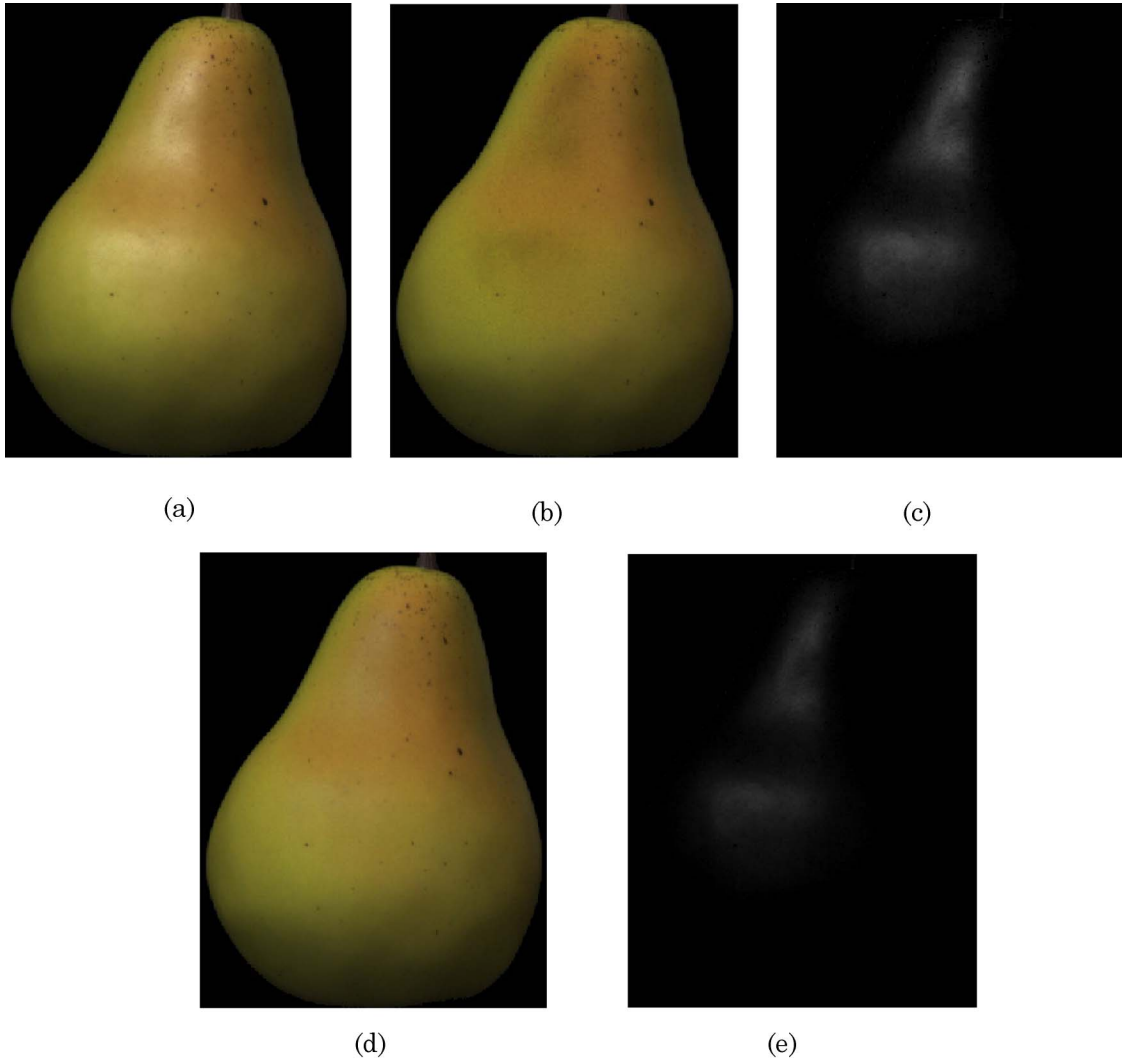
(a)

(b)

(c)

(d)

(e)

Fig. 2. (Color online) Effect of scale k. (a) Original yellow pear image; (b), (c) separated diffuse and specular components with $k = 1$; (d), (e) separated diffuse and specular components with calculated $k = 0.64$.

where $V_{b,\min} = \min_i\{V_{b,i}\}$, Eq. (6) becomes

$$V_{\mathrm{SF},i}(p) = \alpha(p)(V_{b,i} - V_{b,\min}). \qquad (8)$$

It is observed from Eq. (8) that the SF image does not contain the geometrical factor $\beta(p)$ any more. It is noted from Eq. (6) that at least one value of $V_{\mathrm{SF},i}(p)$ is 0 for the three channel, and, as a consequence, the color of the SF image appears darker than that of the original image. The SF images of Tan and Ikeuchi's method [8] and the proposed method are shown in Fig. 1.

The SF image and the actual diffuse reflection of the original image can be related as follows:

$$V_{df,i}(p) = V_i(p) - \beta_s(p) = V_{\mathrm{SF},i}(p) + V_{\min}(p) - \beta_s(p)$$
$$= V_{\mathrm{SF},i}(p) + \tau_s(p), \qquad (9)$$

where $\tau_s(p) = V_{\min}(p) - \beta_s(p)$ is the offset of pixel p. The exact value of $\tau_s(p)$ is unknown before component separation, as it is related to the term $\beta_s(p)$.

It is always desired that the SF image be close to the diffuse component of the original image. In this regard, we propose the concept of the modified specular-free (MSF) image by adding an offset $\tau(p)$ to the SF image:

$$V_{\mathrm{MSF},i}(\tau, p) = V_{\mathrm{SF},i}(p) + \tau(p)$$
$$= \alpha(p)(V_{b,i} - V_{b,\min}) + \tau(p). \qquad (10)$$

It is noted that, compared with the MSF image introduced by Shen $et\ al.$ [11], the offset $\tau(p)$ here not a constant, but is pixel dependent.

The chromaticity of the ith channel for the MSF image is then calculated as

$$c_{\mathrm{MSF},i}(p) = \frac{V_{\mathrm{MSF},i}}{\sum_i V_{\mathrm{MSF},i}} = \frac{\alpha(p)(V_{b,i} - V_{b,\min}) + \tau(p)}{\alpha(p)\sum_i(V_{b,i} - V_{b,\min}) + 3\tau(p)}.$$
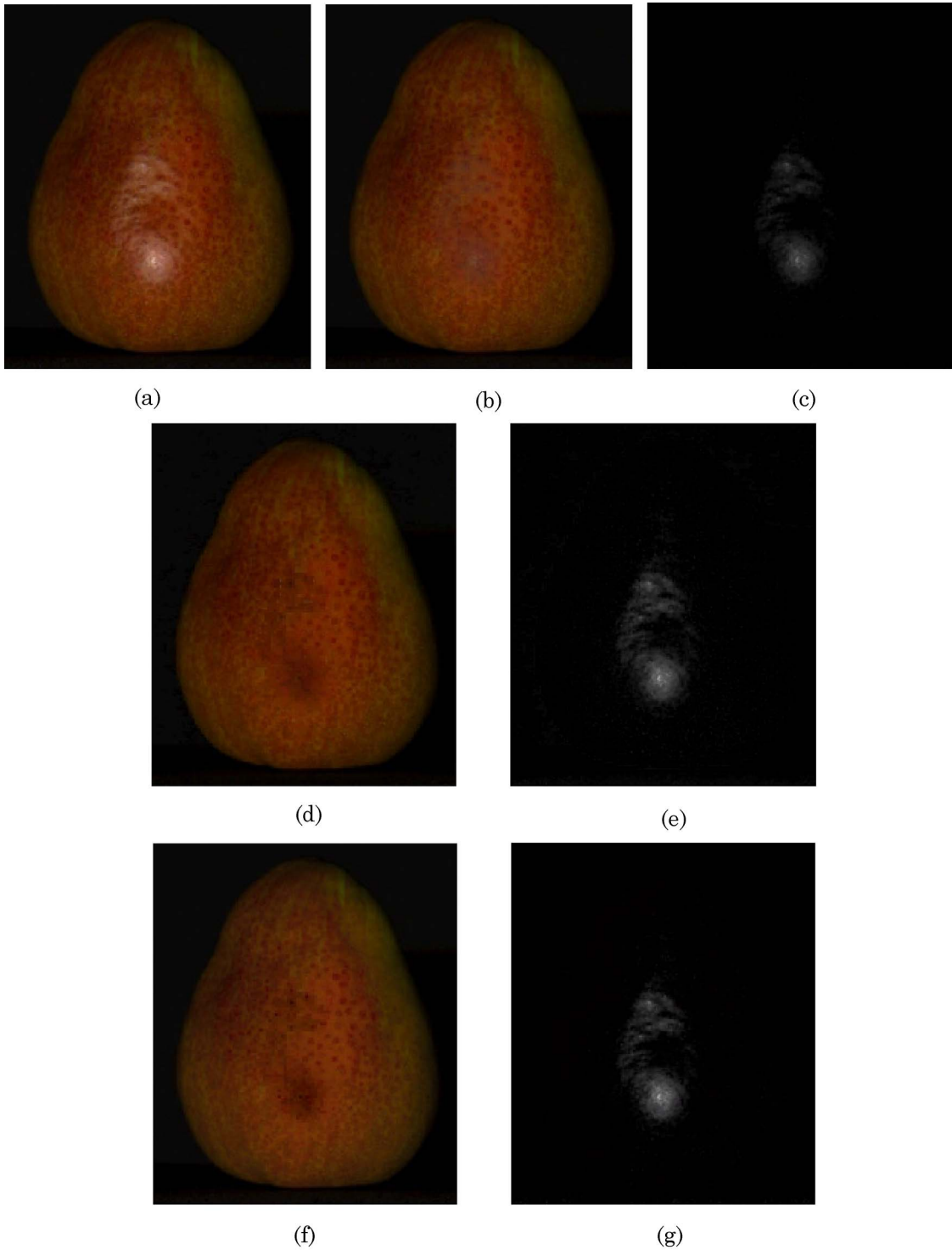$$(11)$$

Fig. 3. (Color online) Separation results of a red pear image. (a) Original image; (b), (c) reflection components by the proposed method; (d), (e) reflection components by Tan's method [8]; (f), (g) reflection components by Shen's method [11].

It is clear that, when the offset $\tau(p)$ does not equal 0, the chromaticity is not independent of the geometrical factor $\alpha(p)$.

In our proposed method, the offset $\tau(p)$ is determined with regard to a threshold that can generally distinguish pixels with highlight. Let T_v denote the threshold, which is calculated as follows:

$$T_v = \mu_v + \eta\sigma_v, \qquad (12)$$

where μ_v and σ_v are the mean and the standard deviation of $V_{\min}(p)$ for all pixels. η is related to the specular degree of an image, and $\eta = 0.5$ is appropriate for most images. If the minimum value of a pixel is smaller than T_v, it should be a diffuse pixel;
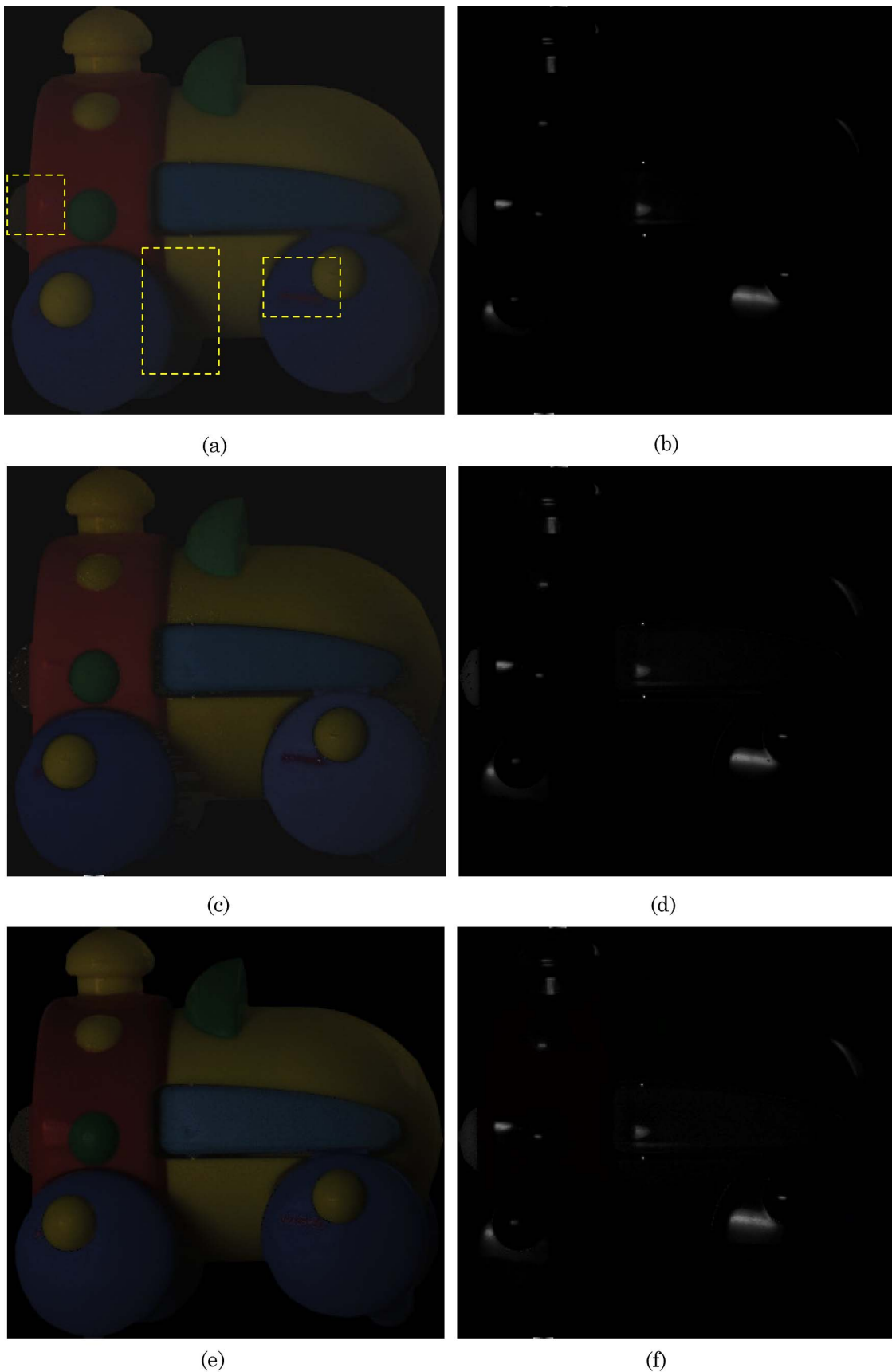
Fig. 4. (Color online) Separation results of the train image. (a), (b) reflection components by the proposed method; (c), (d) reflection components by Tan's method [8]; (e), (f) reflection components by Shen's method [11]. The yellow-dashed rectangles indicate the obvious improvement of the proposed method over the other two methods.
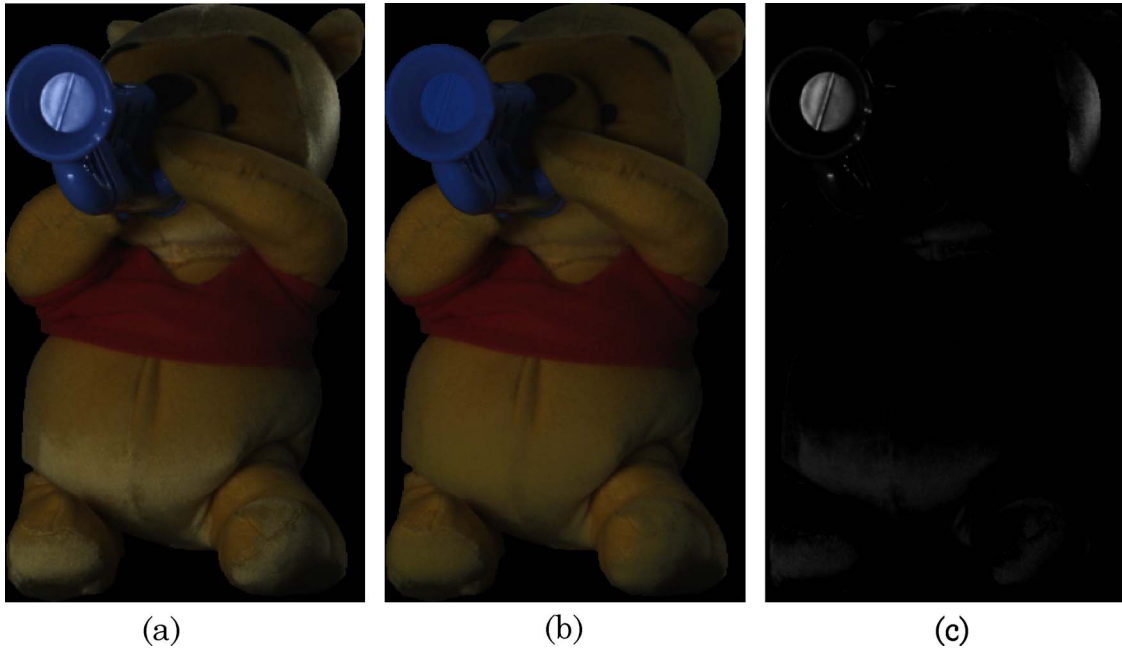
Fig. 5. (Color online) Separation results of a bear image. (a) Original, (b) diffuse component, (c) specular component.

otherwise, it is regarded as a specular candidate. Consequently, the offset $\tau(p)$ is determined as follows:

$$\tau(p) = \begin{cases} T_v & \text{if } V_{\min}(p) > T_v \\ V_{\min}(p) & \text{otherwise} \end{cases}. \qquad (13)$$

It is noted that the specular candidates are the pixels with relatively large RGB values, but some of them may not contain specular reflections. In the following calculation, the specular composition of each specular candidate will be determined.

B. Separation of Specular Reflection Component

In the dichromatic reflection model, the chromaticity of a pixel after specularity removal should be equal to that of the corresponding body color [8,11]. If we assume that the MSF image is similar to the diffuse image, $c_{\text{MSF},i}(p)$ should be close to the chromaticity of the diffuse component $c_{df,i}(p)$, and then we have the following relationship:

$$c_{\text{MSF},i}(\tau,p) \approx c_{df,i}(p) = \frac{V_i(p) - \hat{\beta}_s(p)}{\sum_i V_i(p) - 3\hat{\beta}_s(p)}. \qquad (14)$$

By comparing Eqs. (11) and (14), we can find that $\hat{\beta}_s(p) = V_{\min}(p) - \tau(p)$. As $\hat{\beta}_s(p)$ is related to a constant threshold T_v, it should be similar to the actual specular component but is not the same. More specifically, the specular component is actually $k(p)\hat{\beta}_s(p)$, with $k(p)$ being an adjustment scale at pixel p. Our investigation found that a single scale k is sufficient for adjusting all pixels in an image.

The diffuse reflection component of pixel p is then calculated as

$$\hat{V}_{df,i}(p) = V_i(p) - k\hat{\beta}_s(p). \qquad (15)$$

The scale k is used to adjust the specularity level so that the obtained diffuse component is smooth and natural over the whole image.

The value of k is calculated under the fact that the color intensity is smooth along the boundary between
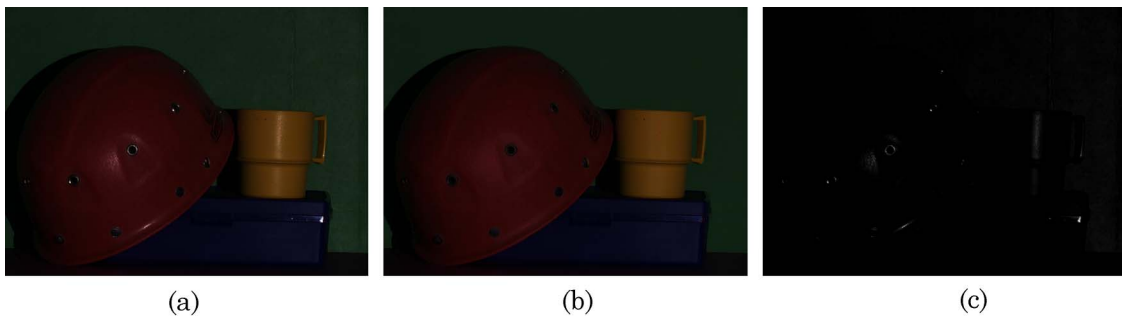

Fig. 6. (Color online) Separation results of a helmet image. (a) Original, (b) diffuse component, (c) specular component.
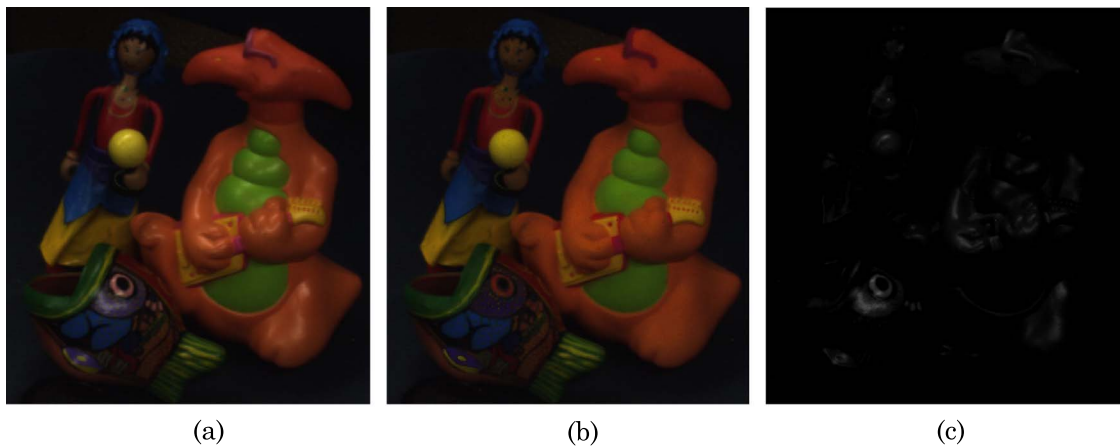
Fig. 7. (Color online) Separation results of a toys image. (a) Original, (b) diffuse component, (c) specular component.

highlight and diffuse regions. After the specularity of each pixel is obtained as described in Eq. (14), the largest region of highlight is located and labeled as the dominant region. The dominant region is then dilated by 5 pixels to obtain its surrounding region. The mean diffuse colors of the dominant and the surrounding region are then set to be equal under the criterion of smooth color transition:

$$\bar{V}_{\text{dom},i} - k\bar{\beta}_{s,\text{dom}} = \bar{V}_{\text{sur},i} - k\bar{\beta}_{s,\text{sur}}, \qquad (16)$$

where $\bar{V}_{\text{dom},i}$ and $\bar{V}_{\text{sur,i}}$ are the mean intensities of dominant and surrounding regions of the ith channel, respectively, and $\bar{\beta}_{s,\text{dom}}$ and $\bar{\beta}_{s,\text{sur}}$ are the mean specular component of the dominant and the surrounding region, respectively. When all three channels (RGB) are considered, the specular scale k can be easily calculated by the least-squares technique.

Figure 2 shows the effect of scale k. The diffuse component of the yellow pear seems unnatural when $k = 1$, as a heavy specular component is subtracted from the original image. With $k = 0.64$ as calculated from Eq. (16), obvious improvement can be obtained. It is worthwhile to note that the calculation of k is not limited to single-colored objects; it can also be applied to a multicolored, textured image provided that the texture distribution in the dominant region is approximately uniform, as will be seen in the experimental results.

4. Experimental Results and Discussion

More than 30 images with different inhomogeneous materials were used in the experiment to evaluate the proposed method. These images were obtained from colleagues, websites, or were acquired ourselves. The proposed method was completed by using the platform of Visual C++ 6.0 on a personal computer with an Intel 2.93 GHz CPU and 1 Gbyte of memory.

Tan's method [8] and Shen's method [11] are used for comparison in the experiment. The source code of Tan's method is freely available on the author's website. Figure 3 compares these three methods on a red

pear image. Tan's and Shen's methods both detect heavy specular components, and therefore the corresponding areas in the diffuse components appear dark. In comparison, the components separated by the proposed method are quite good. Figure 4 shows the separation results of a train image. It is observed that the color appearance of the diffuse component of the proposed method is smoother than that of Tan's and Shen's methods, especially in the three labeled regions. Although the separated diffuse component of the right wheel is not perfect in the proposed method, it is still better than those of the competing methods. Figures 5–7 illustrate the results of the proposed method on different images. For the bear image in Fig. 5, the strong specularity on the horn is handled quite well. In Fig. 6, the strong specularity on the blue box and the relatively weak specularity on the yellow cup and red helmet are all satisfactorily decomposed. The reflection separation task is quite challenging for the toys image in Fig. 6. The image contains several plastic objects with different colors and textures, and the highlights are widely distributed. The successful separation results further verified the effectiveness of the proposed method.

In additional to the separation accuracy, the running speed is also an important issue when evaluating the performance of the methods. In Tan's method [8], the specularity intensity of a pixel is gradually reduced, based on a diffuse pixel verification process and a specularity reduction process. The

Table 1. Running Times of Three Methods

Image	Size (pixels)	Tan's Method [8]	Shen's Method [11]	Proposed
		Running Time (s)		
Yellow pear	276×360	7.25	0.16	0.08
Red pear	200×238	4.80	0.06	0.03
Train	332×309	8.44	0.38	0.09
Bear	369×461	13.11	0.49	0.13
Helmet	637×468	54.27	1.34	0.31
Toys	353×387	21.20	0.75	0.19

computation is relatively heavy as the loop of specularity reduction terminates only when the maximum chromaticities of all pixels in a single-colored surface are the same. In the iterative framework of Shen's method [11], an appropriate diffuse pixel is chosen, and then specularity levels of the pixels with close MSF chromaticity are solved under the least-squares criterion. This iterative process continues until all the nondiffuse pixels are dealt with. In comparison, the proposed method does not involve any iterative process, and thus the computation should be much efficient. As expected, Table 1 indicates that the running speed of the proposed method is about 100 times faster than that of Tan's method [8] and at least 2 times faster than that of Shen's method [11]. By using an up-to-date computer system and code optimization, it is possible for the proposed method to run in real time.

5. Conclusion

This paper proposes a new method for separating diffuse and specular reflection components in a single image. A MSF image is generated from the original image by subtracting the minimum of RGB values and adding a pixel-dependent offset for each pixel. The specular component is then adjusted under the criterion of smooth color transition along the boundary of highlight and surrounding regions. In such a way, the separation of reflection components is handled on individual pixel level, without any image segmentation or local interactions between pixels. Experimental results indicate that the proposed method outperforms the existing technique in terms of both running speed and separation accuracy.

References

1. S. Lin and S. W. Lee, "Estimation of diffuse and specular appearance," in *International Conference on Computer Vision (ICCV)* (IEEE, 1999), pp. 855–860.
2. K. Hara, K. Nishino, and K. Ikeuchi, "Determining reflectance and light position from a single image without distant illumination assumption," in *International Conference on Computer Vision (ICCV)* (IEEE, 2003), Vol. 1, pp. 560–567.
3. J. H. Xin and H. L. Shen, "Accurate color synthesis of three-dimensional objects in an image," J. Opt. Soc. Am. A **21**, 713–723 (2004).
4. S. A. Shafer, "Using color to separate reflection components," Color Res. Appl. **10**, 210–218 (1985).
5. H. C. Lee, D. J. Breneman, and C. O. Schulte, "Modeling light reflection for computer color vision," IEEE Trans. Pattern Anal. Mach. Intell. **12**, 402–409 (1990).
6. S. K. Nayar, X. S. Fang, and T. Boult, "Separation of reflection components using color and polarization," Int. J. Comput. Vis. **21**, 163–186 (1997).
7. G. J. Klinker, S. A. Shafer, and T. Kanade, "The measurement of highlights in color images," Int. J. Comput. Vis. **2**, 7–32 (1988).
8. R. T. Tan and K. Ikeuchi, "Separating reflection components of textured surfaces using a single image," IEEE Trans. Pattern Anal. Mach. Intell. **27**, 178–193 (2005).
9. D. Miyazaki, R. T. Tan, K. Hara, and K. Ikeuchi, "Polarization-based inverse rendering from a single view," in *International Conference on Computer Vision (ICCV)* (IEEE, 2003), Vol. 2, pp. 982–987.
10. K. J. Yoon, Y. J. Choi, and I. S. Kweon, "Fast separation of reflection components using a specularity-invariant image representation," in *International Conference on Image Processing (ICIP)* (IEEE, 2006), pp. 973–976.
11. H. L. Shen, H. G. Zhang, S. J. Shao, and J. H. Xin, "Chromaticity-based separation of reflection components in a single image," Pattern Recognit. **41**, 2461–2469 (2008).
12. L. Shen, T. Machida, and H. Takemura, "Efficient photometric stereo technique for three-dimensional surfaces with unknown BRDF," in *the Fifth International Conference on 3-D Digital Imaging and Modeling (3DIM'05)* (IEEE, 2005), pp. 326–333.
13. R. T. Tan, K. Nishino, and K. Ikeuchi, "Separating reflection components based on chromaticity and noise analysis," IEEE Trans. Pattern Anal. Mach. Intell. **26**, 1373–1379 (2004).
14. R. T. Tan and K. Ikeuchi, "Reflection components decomposition of textured surface using linear basis functions," in *Conference on Computer Vision and Pattern Recognition (CVPR)* (IEEE, 2005), Vol. 1, pp. 125–131.
15. S. P. Mallick, T. Zickler, P. N. Belhumeur, and D. J. Kriegman, "Specularity removal in images and videos: a PDE approach," in *9th European Conference on Computer Vision, ECCV 2006*, A. Leonardis, H. Bischof, and A. Pinz, eds., Vol. 3951 of *Lecture Notes in Computer Science* (Springer, 2006), pp. 550–563.
16. S. Mallick, T. Zickler, D. Kriegman, and P. Belhumeur, "Beyond Lambert: reconstructing specular surfaces using color," in *Conference on Computer Vision and Pattern Recognition (CVPR)* (IEEE, 2005) Vol. 2, pp. 619–626.
17. J. W. Park and K. H. Lee, "Inpainting highlights using color line projection," IEICE Trans. Inf. Syst. **E90D**, 250–257 (2007).
18. P. Tan, S. Lin, L. Quan, and H. Y. Shum, "Highlight removal by illumination constrained inpainting," in *International Conference on Computer Vision (ICCV)* (IEEE, 2003), pp. 164–169.
19. K. Barnard, V. Cardei, and B. Funt, "A comparison of computational color constancy algorithms. I: methodology and experiments with synthesized data," IEEE Trans. Image Process. **11**, 972–984 (2002).